Identification of an E-selectin Region Critical for Carbohydrate Recognition and Cell Adhesion

David V. Erbe,* Barry A. Wolitzky,‡ Leonard G. Presta,§ Christine R. Norton,‡ Robert J. Ramos,‡ Daniel K. Burns,‡ John M. Rumberger,‡ B. N. Narasinga Rao,‖ Carrol Foxall,‖ Brian K. Brandley,‖ and Laurence A. Lasky*

Departments of *Immunology and §Protein Engineering, Genentech, Inc., South San Francisco, California 94080; ‡Department of Molecular Genetics, Roche Research Center, Hoffmann-La Roche Inc., Nutley, New Jersey 07110; and ‖Glycomed, Inc., Alameda, California 94501

Abstract. E-selectin elicits cell adhesion by binding to the cell surface carbohydrate, sialyl Lewis X (sLe^x). We evaluated the effects of mutations in the E-selectin lectin domain on the binding of a panel of anti–E-selectin mAbs and on the recognition of immobilized sLe^x glycolipid. Functional residues were then superimposed onto a three-dimensional model of the E-selectin lectin domain. This analysis demonstrated that the epitopes recognized by blocking mAbs map to a patch near the antiparallel beta sheet derived from the NH_2 and COOH termini of the lectin domain and two adjacent loops. Mutations that affect sLe^x binding map to this same region. These results thus define a small region of the E-selectin lectin domain that is critical for carbohydrate recognition.

THE selectins are three cell adhesion molecules that are unified structurally by the inclusion of lectin, EGF-like and complement binding-like domains (4, 26, 34, 51, 54) and functionally by their ability to mediate cell binding through interactions between their lectin domains and cell surface carbohydrate ligands (8, 53). L-selectin is found on leukocytes and is involved with the trafficking of lymphocytes to peripheral lymphoid tissues (20) and with acute neutrophil-mediated inflammatory responses (62). It appears to recognize an unknown sialylated, fucosylated, sulfated carbohydrate ligand(s) on at least two endothelial glycoproteins (24, 57), one of which has recently been cloned (35). E-selectin is an endothelial adhesion molecule that is induced by various inflammatory stimuli (3, 28, 40) and that recognizes the neutrophil and monocyte cell surface carbohydrate, sialyl Lewis x (sLe^x)[1] (39, 43, 56, 60). In addition, E-selectin may also be involved with the recognition of an sLe^x-like carbohydrate on the surface of a skin-homing subset of lymphocytes (44, 50). The minimum-sized sLe^x-related carbohydrate recognized by E-selectin is a tetrasaccharide of the structure Sialic Acid α2–3 Galactose β1–4 (Fucose α1–3) *N*-Acetyl Gluclosamine (58). P-selectin is found in alpha granules of platelets and Weible-Palade bodies of endothelial cells (5, 41). Its surface expression is induced within minutes of exposure to thrombin, substance P, histamine, or peroxide, and it appears to recognize a carbohydrate that is either identical to or closely related to sLe^x on both neutrophil and monocyte cell surfaces (31, 32, 42, 46). In the case of all three selectins, the adhesive interactions require α2–3-linked sialic acid, while in the case of E-selectin, and probably P-selectin, the recognition event also requires a fucose residue (8, 53, 58). The adhesive interactions between selectins and their carbohydrate ligands may be relatively weak, since L-selectin and P-selectin have been shown to be involved in the relatively low affinity "rolling" of leukocytes along the endothelium during inflammatory responses (9, 36, 38, 59).

The molecular details of the interactions between selectins and their carbohydrate ligands are poorly understood. The fact that selectins require sialic acid for adhesion, when coupled with the finding that certain negatively charged carbohydrate polymers (fucoidin, dextran sulfate, and polyphosphomannan ester) are effective inhibitors of some selectin-mediated cell adhesion, is consistent with the involvement of positively charged amino acids in carbohydrate recognition (24, 42, 46, 57, 58, 69). However, such protein-sialic acid interactions can be accomplished by noncharged side chains. Crystallographic analysis of the low-affinity interaction between the influenza hemagglutinin glycoprotein, which is not related to type C lectins, and its ligand, sialic acid, revealed that this interaction involves diverse amino acid side chains, none of which are positively charged (66). That a simple face or pocket of E-selectin, and potentially P-selectin (46), is involved with recognition of sLe^x is suggested by nuclear magnetic resonance (NMR) solution analyses of sLe^x structure. This analysis demonstrated that the critical sialic acid and fucose residues both point to one face of this

D. V. Erbe and B. A. Wolitzky contributed equally to this study.

1. *Abbreviations used in this paper*: DPBS, Dulbecco's PBS; HUVEC, human umbilical vein endothelial cell; MBP, mannose-binding protein; sLe^x, sialyl Lewis x.

carbohydrate ligand and are separated by ~10 Å, while an inactive form of this carbohydrate (with 2–6 linked sialic acid) has these two components pointing in different directions (1, 58). A similar structural analysis of another ligand for E-selectin, sialyl Lewis a (sLe^a: Sialic Acid α2–3 Galactose β1–3 (Fucose α1–4) *N*-Acetyl Glucosamine), has revealed that the critical sialic acid and fucose residues again point to one face of the tetrasaccharide and are separated by approximately the same distance as in sLe^x (1, 58). These results are all consistent with the recognition of sLe^x by a relatively small region of E-selectin.

To analyze the adhesive interactions between sLe^x and E-selectin on a more detailed level, we have undertaken two strategies. First, chimeric human–rabbit lectin domains have been generated based upon amino acid sequence differences between the two species. These chimeras have then been used to map epitopes recognized by blocking antibodies to human E-selectin. Second, E-selectin mutants with alanine substitutions have been generated and analyzed for binding to a panel of blocking and nonblocking antibodies and for their ability to adhere to immobilized sLe^x glycoplipid. Residues affecting various aspects of E-selectin structure and/or function have then been superimposed onto a three-dimensional model of the E-selectin lectin domain generated using the structural coordinates determined for a related C-type lectin, the mannose binding protein (67). Together, these data point to a relatively small region of the E-selectin lectin domain that is critical for recognition of sLe^x.

Materials and Methods

Production and Characterization of Anti–E-selectin mAbs

mAbs to both human and rabbit E-selectin were generated by immunization of mice with COS cells transiently expressing E-selectin. COS cells (5×10^7/0.8 ml in Dulbecco's PBS (DPBS) were transfected by electroporation (350 V, 250 μF, Bio-Rad Gene Pulser) with 20 μg human or rabbit E-selectin cDNA, incubated on ice for 10 min, resuspended in DME/10% FBS and plated at 10^7 cells per 225-cm^2-tissue culture flask. Transfected cells were harvested nonenzymatically at 48–72 h, washed twice, and resuspended in DPBS. Mice were routinely immunized i.p. with 1×10^7 cells and boosted every 2–3 wk. Hybridomas were produced by fusion of immunized mouse splenocytes with SP2/0 cells using standard techniques (19). Hybridoma supernatants were screened by a differential binding ELISA to Immulon 2 microtiter plates (Dynatech Laboratories, Inc., Chantilly, VA) coated with detergent extracts of membranes from E-selectin transfected and control/nontransfected COS cells. Crude membrane fractions were extracted in 2% Triton X-100, 150 mM NaCl, 50 mM Tris, pH 7.5 (2.5×10^8 cell equivalents/ml). Extracts were diluted in 50 mM Na2CO3, pH 9.6, and directly coated onto assay plates. Anti-human antibodies were also screened by ELISA for selective binding to human umbilical vein endothelial cells (HUVECs) treated for 4 h with rhIL-1α (550 pg/ml) and rhTNF (400 U/ml) compared with untreated HUVECs. The specificity of these mAbs were confirmed with cytokine treated HUVECs, and transiently transfected COS cells by immunoblotting, immunoprecipitation, and indirect immunofluorescence.

mAbs 7H5 (IgG3), 8E4 (IgG2A), 3B7 (IgG1), 1D6 (IgG1), 4D9 (IgG3), 1E5 (IgG1), 9A1 (IgG1), 7E10 (IgG1), and 1B3 (IgM) were generated to human E-selectin, while mAbs 14G2 (IgG1), 11G5 (IgM), and 9H9 (IgM) were produced to rabbit E-selectin. Ascites was produced by standard techniques (23) and antibodies were purified by the caprylic acid precipitation method as described (48). mAbs BBA 1 and BBA 2 were purchased from British Biotechnology (Oxford, England) while mAb ENA-1 was purchased from San Bio (Uden, Netherlands).

Adhesion Assays

Confluent cultures of HUVECs plated onto gelatin-coated 96-well tissue culture plates (Costar Corp., Cambridge, MA) were treated for 4 h with rhIL-1α (550 pg/ml) and rhTNF (400 U/ml). Wells were washed three times with DPBS and incubated for 1 h at 37°C in DPBS containing 1% BSA and 10 μg/ml of designated mAb. HL60 cells were washed twice and resuspended in RPMI Medium 1640 (Gibco Laboratories, Grand Island, NY) at 5×10^6 cells/ml and labeled for 30 min at 37°C with 40 μg/ml 6 Carboxyfluorescein (6-CFDA). 6-CFDA loaded HL60 cells (100,000 cells per well) were added and incubated for 20 min at 25°C. Wells were filled with RPMI and plates were sealed, inverted, and spun for 6 min at 500 *g*. Nonadherent cells were removed by aspiration and plates read in a CytoFluor 2300 fluorescent plate reader (Millipore Corp., Bedford, MA.).

COS cells were plated at 5×10^5 cells per 35-mm-diam well 18 h before transfection. Cells were washed with DPBS and 2 μg DNA was added in 1 ml DME containing 10% Nutridoma (Boehringer-Mannheim Corp., Indianapolis, IN), 50 μM chloroquine, and 500 ng/ml DEAE dextran. After incubation for 2.5 h at 37°C, the wells were aspirated and the cells were incubated in Iscove's modified Dulbecco's medium (IMDM) containing 10% FBS and 10% DMSO for 2.5 min. Wells were aspirated and cells grown in IMDM containing 10% FBS at 37°C for 48–72 h. For adhesion assays, 5×10^6 6-CFDA loaded HL60 cells were added to each 35-mm-diam well and incubated for 30 min at 25°C. Wells were washed 3 times with RPMI and the fluorescence associated with adherent cells determined in the CytoFluor 2300 plate reader.

Indirect Immunofluorescence

Transiently transfected COS cells were fixed in DPBS containing 1% (wt/vol) formaldehyde for 15 min at 25°C. After two washes with DPBS, the cells were blocked with DPBS containing 10% horse serum (DPBS/10% HS) for 30 min at room temperature. Cells were incubated for 30 min with 5 μg/ml mAbs 387, 8E4, 7H5, or 14G2 in DPBS/10% HS and then washed three times with DPBS. After a 30-min incubation with rhodamine-conjugated goat anti-mouse IgG, cells were washed with DPBS, and fluorescence observed on a Zeiss Axioskop microscope (Carl Zeiss, Inc., Thornwood, NY).

Human–Rabbit Chimeric E-selectin Constructs

Expression of truncated forms of human and rabbit E-selectin on the surface of COS cells was achieved by fusing the selectin sequences with the carboxy-terminal 37 amino acids of CD16 which contains the signal sequence for cell surface anchorage via a glycosylphosphatidylinositol (GPI) linkage (49). All E-selectin fragments were generated by polymerase chain reaction (PCR) and cloned into the plasmid vector pBC12BI (11) that had been modified to contain the CD16 sequences. Recombinant genes were expressed using the initiating Met codon from the rat preproinsulin gene in pBC12BI and the primary translation product contains five amino acids derived from the insulin signal sequence. The human lectin-EGF construct contained amino acids −15 through +157 (4), the rabbit lectin-EGF contained residues −17 through +156 (30), while the HuRa-1 contained amino acids −15 to +9 of human E-selectin contiguous with residues 10 through 156 of rabbit E-selectin. The CD16 sequences required for GPI anchorage to the cell surface were fused to the carboxy termini of each construct.

Construction and Expression of E-selectin–IgG Chimera Mutants

Production and characterization of the E-selectin–IgG chimera has been previously described (18). Mutations were introduced into the lectin domain of this chimera by the method of Kunkel (29) using the Muta-Gene Phagemid in vitro Mutagenesis Kit (BioRad Laboratories, Richmond, CA) according to the manufacturer's instructions. Correct mutants were confirmed by sequencing and the mutant chimeras were transiently expressed and secreted by transfection of 293 cells (63). The concentration of each chimera in the resultant supernatants were then quantified by ELISA using an anti-human IgG1-Fc specific mouse mAb as previously described (61). Mutation sites are defined using the following nomenclature: K113A is a mutant where the lysine (K) at position 113 is changed to an alanine (A).

mAb Binding of E-selectin–IgG Mutants

Reactivity of the mutant E-selectin–IgG chimeras with the various antibodies was determined using a previously described ELISA format (61) in which the purified mAbs were coated onto microtiter wells, then blocked with BSA. 293 cell supernatants containing equal concentrations of wild-type or mutant chimeras were incubated in the wells, followed by washing

and detection of the captured chimeras with HRP-conjugated goat polyclonal anti-human Fc antibody.

sLe^x Binding of E-selectin-IgG Mutants

Assays for binding of the mutant E-selectin-IgG chimeras to immobilized sLe^x glycolipids were performed essentially as described (18). Briefly, sLe^x glycolipids were dried onto microtiter wells, washed with distilled water, and then blocked with BSA. Biotinylated goat anti-human IgG Fc and alkaline phosphatase-streptavidin (CALTAG Laboratories, South San Francisco, CA) were each diluted 1:1,000 into 293 cell supernatants containing equal concentrations of wild-type or mutant chimeras and allowed to form a complex before addition to the wells. These supernatants were then incubated on the sLe^x glycolipid-coated surfaces, followed by washing, addition of substrate (*p*-nitrophenyl phosphate), and measurement of the OD at 405 nm.

Generation of a Model of the E-selectin Lectin Domain

The model of E-selectin was generated based on the crystal structure of the rat mannose-binding protein (MBP) (67). The sequence of E-selectin was aligned with those of mouse L-selectin (LHR) (34) and MBP using the alignment of the latter two proteins provided (67). Eleven insertions and two deletions in E-selectin relative to MBP mapped to four surface loops in the MBP structure. MBP (molecule 1) was transformed into E-selectin in three steps. First, all residues except those involving insertions/deletions were changed to the E-selectin sequence using the INSIGHT-II program (Biosym Technologies, San Diego, CA). If possible, conformations of E-selectin sidechains were kept similar to those of MBP, otherwise they were based on rotamer libraries (47), packing and hydrogen-bonding considerations. Second, possible loop structures for the E-selectin insertions/deletions were gleaned from a search of crystal structures in the Protein Data Bank (2) using the INSIGHT-II program. Third, each of the 30 water molecules present in the MBP crystal structure was evaluated regarding its retention in the E-selectin model. Only seven waters were included in the E-selectin model, four of which corresponded to MBP water molecules 23, 24, 25, and 30.

The E-selectin model was subjected to 6,000 cycles of energy minimization using the DISCOVER program (Biosym Technologies). The all-atom AMBER forcefield (64, 65) was used for all calculations, using a 14Å cutoff for nonbonded interactions and a linear dielectric ($\epsilon = 4.0$*r). Hydrogen atoms were added to the structure using INSIGHT-II and positions of hydrogens on Ser, Thr, and Tyr sidechains and on water molecules were checked visually for proper alignment in hydrogen bonds, if present. Energy minimization was performed in six stages of 1,000 cycles each. In stage 1, steepest-descents minimization was used with Cα atoms of residues S2-V27, Q30-S40, Y49-R54, W60-V61, N75-N82, E88-I93, and W103-T119 constrained to their initial positions using a force constant of 100 kcal/Å. 105 hydrogen-bond constraints (50 kcal/mol) were also invoked involving primarily hydrogen bonds between residues in the β strands and α helices. This allowed loop structures and sidechains to move while preserving the integrity of the secondary structure present in the E-selectin model. In stages 2 and 3, the Cα tether force constant was reduced to 50 and 10 kcal/Å, respectively, and conjugate gradients minimization was used. In stages 4 and 5, the Cα constraints were released and, finally, in stage 6 the hydrogen-bond constraints were released. The MBP crystal structure includes two Ho^{2+} ions which occupy the two Ca^{2+}-binding sites in MBP. E-selectin retains one Ca^{2+}-binding site, but loses the second (see Results). Since the AMBER forcefield (64, 65) does not include a representation for Ca^{2+}, the Ca^{2+} atom was removed and the sidechains which coordinate the Ca^{2+} (E80, N82, E88, N105, D106) were fixed throughout the minimization procedure.

Results

Characterization of a Panel of E-selectin Antibodies

To facilitate the study of E-selectin structure and function, we generated a panel of blocking and nonblocking mAbs directed against human and rabbit E-selectin (see Materials and Methods). Three anti-human E-selectin mAbs (7H5, 8E4, and 3B7) were found to inhibit the adhesion of HL60 cells to cytokine activated HUVECs and E-selectin transfected COS cells (Fig. 1 *A*). Cross-reactivity studies demonstrated that these three blocking mAbs did not recognize rabbit E-selectin (Fig. 1 *B*), a result that facilitated mapping of the epitopes recognized by these mAbs (see below). The commercially available anti-human E-selectin mAbs, BBA1, BBA2, and ENA-1, also did not cross react with rabbit E-selectin. (Fig. 1 *B*). While none of these three commercial mAbs significantly blocked E-selectin-mediated HL60 adherence in our cell adhesion assay (Fig. 1 *A*), BBA2 has clear adhesion blocking activity in assays done at low temperature (45) and ENA-1 has been shown to block neutrophil adhesion to activated HUVECs (37). Furthermore, BBA2 and ENA-1 both effectively inhibit binding of E-selectin to immobilized sLe^x glycolipid (18). Since sLe^x is the major carbohydrate ligand for E-selectin on the leukocyte cell surface, it seemed

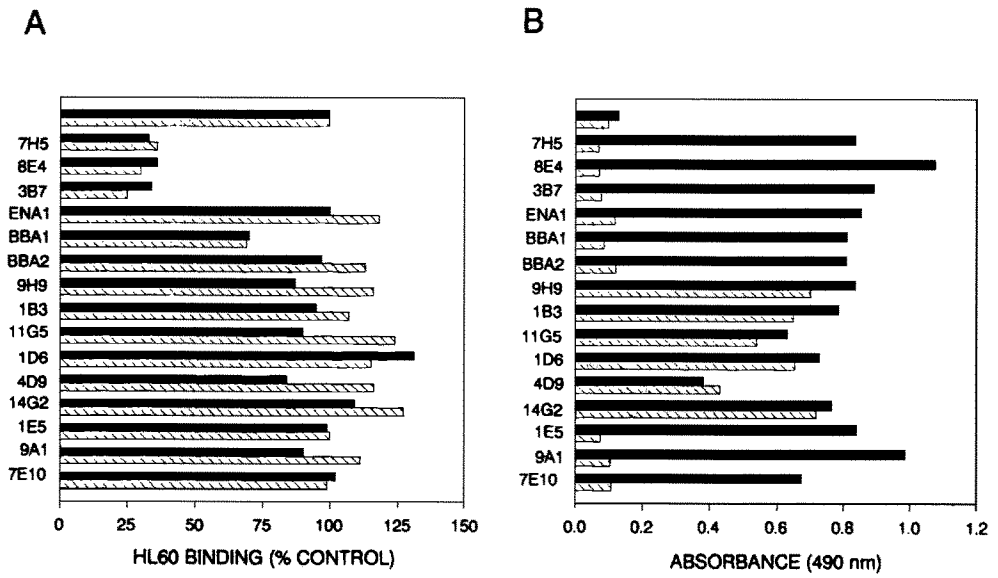

Figure 1. Characterization of anti-E-selectin mAbs. (*A*) Inhibition of HL60 cell adhesion to cytokine activated HUVECs (■) and E-selectin transfected COS cells (▨) by anti-E-selectin mAbs. Cells were preincubated with mAbs (10 μg/ml) for 1 h at room temperature and HL60 cell adhesion determined as described in Materials and Methods. Each bar represents the mean of triplicate determinations expressed as a percent of control binding. Antibody treatments resulting in <40 percent of control adhesion were scored as blocking in these assays. (*B*) Binding of anti-E-selectin mAbs to human (■) and rabbit (▨) E-selectin. Antibodies (10 μg/ml) were incubated for 1 h at room temperature on 96-well microtiter plates to which recombinant soluble human or rabbit E-selectin had been bound. Wells were washed and incubated with HRP-coupled goat anti-mouse IgG, washed, and developed using standard protocols.

likely that analysis of the epitopes recognized by this panel of blocking antibodies (7H5, 8E4, 3B7, BBA2 and ENA-1) might indicate region(s) of E-selectin involved with carbohydrate recognition and resultant cell adhesion. In addition, the mapping of regions recognized by nonblocking mAbs should confirm the site(s) found for blocking antibodies by indicating regions not involved with carbohydrate binding. Therefore, the initial step in analyzing the regions of E-selectin involved in carbohydrate interactions consisted of mapping the epitopes recognized by blocking and nonblocking mAbs.

Analysis of E-selectin mAb Binding

The E-selectin mutagenesis strategy was driven by two major considerations. The first consideration derived from previous work which localized the epitope recognized by blocking mAb, Mel 14, to the NH_2-terminal 53 amino acids of L-selectin (6). Additional mapping showed that part of the Mel 14 epitope was found within the first eight amino acids (D. Erbe, unpublished data). One prediction of this result is that blocking mAbs directed against E-selectin may also recognize the lectin domain NH_2 terminus. A second strategy targeted positively charged residues in the lectin domain of E-selectin. These residues could contribute significantly to binding due to the previously mentioned possibility that a basic side chain may form a salt bridge with the sialic acid carboxylate, and due to the fact that hydrogen bonds involving charged residues contribute more to binding affinity than those involving uncharged residues (7, 17). Finally, charged amino acids are usually found on protein surfaces where they play a prominent role in antigenic epitopes (25, 52).

As described above, none of the anti-human E-selectin blocking mAbs reacted with rabbit E-selectin. Comparison of the amino acid sequences of the lectin domains of human and rabbit E-selectin showed that 5 of 16 differences were clustered in the NH_2-terminal nine amino acids (Fig. 2 *A*). To determine whether blocking mAbs map to this region, a chimeric protein containing rabbit E-selectin lectin and EGF-like domains with the NH_2-terminal nine amino acids replaced by the corresponding sequence from human E-selectin was generated (Hu-Ra-1) (see Fig. 2 *B*). This construct was produced as a fusion of the lectin and EGF-like domains with a region of CD16 sufficient to allow anchoring of the expressed protein to the cell surface by a glycosyl-inositol phosphate linkage (Fig. 2 *B*). The EGF-like domain was included because previous data suggested that the conformation of selectin lectin domains required an adjacent EGF-like domain (6, 60). Indirect immunofluorescence on COS cells transfected with human lectin-EGF-CD16, rabbit lectin-EGF-CD16, or the human-rabbit chimera (Hu-Ra-1) demonstrated that human amino acids 1-9 in the rabbit E-selectin background were sufficient to confer mAb 7H5 and 8E4 binding but not mAb 3B7 binding (Fig. 3 *A*). In similar experiments, ENA-1, but not BBA2, bound to HuRa-1 (not shown). In addition, adhesion of HL60 cells to Hu-Ra-1-transfected COS cells was inhibited by mAbs 7H5 and 8E4, but was unaffected by mAb 3B7 or the nonblocking mAb 14G2 (Fig. 4). These data were consistent with the localization of the major antigenic determinants recognized by three blocking mAbs (7H5, 8E4, and ENA-1) to the NH_2-terminal nine amino acids of human E-selectin. A second human-rabbit chimeric

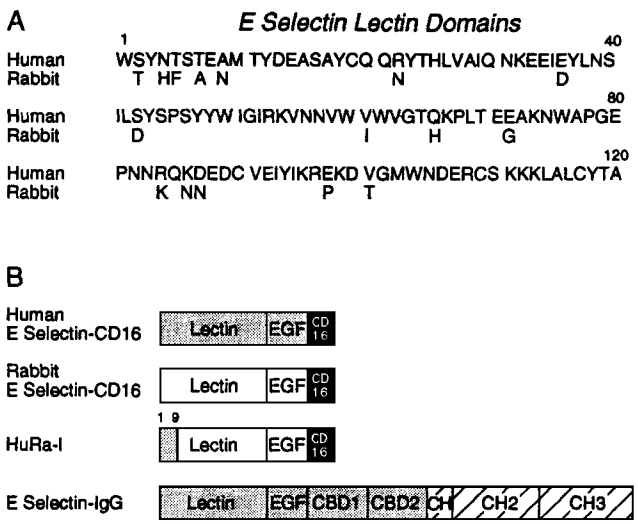

Figure 2. E-selectin constructs. (*A*) Amino acid alignment of the lectin domains of human and rabbit E-selectin beginning at the putative NH_2 terminus of the mature polypeptide. Amino acid substitutions in the rabbit peptide are depicted, all other positions are identical with the human residues. (*B*) E-selectin constructs used to map mAbs and sLe^x binding sites. The human E-selectin contained amino acids 1-157, the rabbit E-selectin encoded amino acids 1-156 and HuRa-1 contained residues 1-9 of human contiguous with residues 10-156 of rabbit E-selectin. Each is anchored to the cell surface via a GPI link encoded by CD16 sequences. Also shown is an E-selectin-IgG chimera (E Sel-IgG) containing the lectin, EGF-like and complement binding-like domains (*CBD*) 1 and 2 of human E-selectin ligated to the hinge, CH2 and CH3 regions of human IgG 1 (61).

E-selectin, HuRa-2, was produced by substitution of rabbit residues with their human counterparts at positions 98 and 101 (P98E and T101V) in the HuRa-1 background. In contrast to the pattern observed with rabbit E-selectin and HuRa-1, COS cells transfected with HuRa-2 did bind mAb 3B7, and adhesion of HL60 cells to these cells was significantly inhibited by mAb 3B7 (Fig. 3 *B*).

To facilitate further mAb mapping and allow for direct carbohydrate binding studies (see below), mutations were introduced into the lectin domain of an E-selectin-human IgG chimera that is similar to a previously described L-selectin-IgG chimera (Fig. 2 *B*) (18, 61). The E-selectin-IgG chimera allowed for easy quantitation of individual mutants by analysis of the amount of human IgG produced from each transient cell transfection assay (see Materials and Methods). The inclusion of the human IgG tail also allowed for rapid analysis of the ability of each mutant to bind the anti-E-selectin antibody panel, as well as to immobilized sLe^x, by use of labeled anti-IgG antibody. In this way, amino acid substitutions which affected global lectin structure (loss of recognition by all mAbs), localized structure (loss of recognition by a subset of mAbs), and carbohydrate recognition (loss of sugar recognition with retention of recognition by most or all mAbs) could be rapidly differentiated (see Table I).

Fig. 5 shows a number of amino acid substitutions that appear to affect the binding of various mAbs to E-selectin. Since the chimeric construct of the lectin domains of human and rabbit E-selectin (HuRa-1) identified the NH_2-terminal

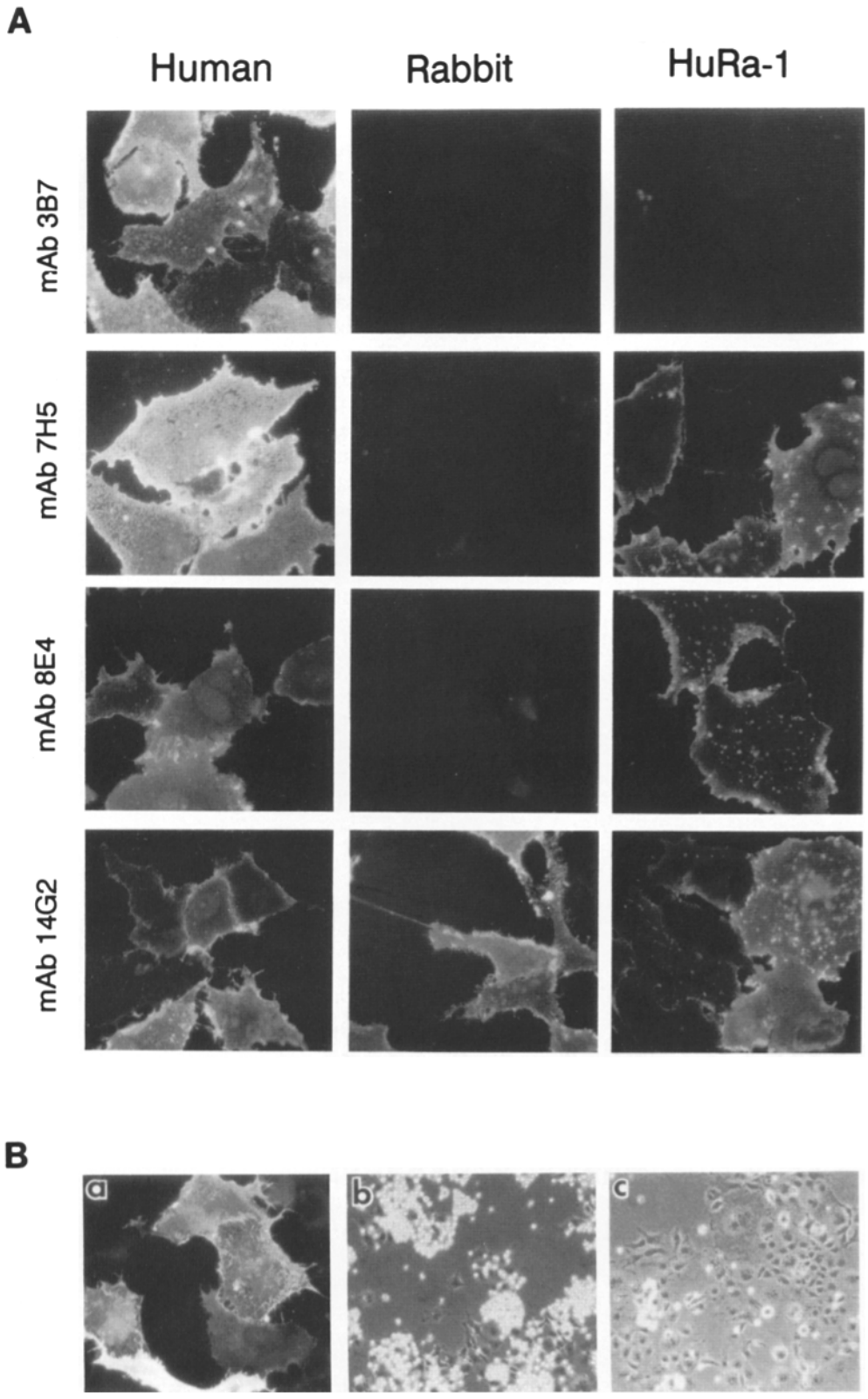

Figure 3. Binding of blocking antibodies to human–rabbit chimeras. (*A*) Immunofluorescence localization of antibody binding to human E-selectin lec-egf-CD16 (column 1), rabbit E-selectin lec-egf CD16 (column 2), and HuRa-1, human–rabbit chimeric E-selectin lectin-egf CD16 (column 3) transfected COS cells. Transfected cells were fixed and stained with mAbs 3B7 (row 1), 7H5 (row 2), 8E4 (row 3), or 14G2 (row 4). (*B*) Binding and inhibition of HL60 cell adhesion to HuRa-2 by mAb 3B7. (*a*) Immunofluorescence localization of antibody 3B7 binding to HuRa-2 transfected COS cells; (*b*) HL60 cell adhesion to HuRa-2 transfected COS cell monolayers; and (*c*) inhibition of HL60 cell adhesion to HuRa-2 by mAb 3B7. Cells were preincubated with mAb 3B7 (10 μg/ml) for 1 h and coincubated with HL60 cells for 30 min at 25°C.

nine amino acids as forming at least part of the epitopes for three blocking antibodies (8E4, 7H5, and ENA-1), we first constructed further mutants within this region, concentrating on the five positions (residues 2, 4, 5, 7, and 9) which differ between rabbit and human. A human E-selectin–IgG chimera in which residues 2, 4, and 5 were mutated retained binding to the entire panel of antibodies, indicating that these amino acids are not critical for mAb binding (Table I). However, a mutation which replaces the human E-selectin amino acids at positions 7 and 9 with their rabbit counterparts resulted in loss of binding of antibodies 7H5, 8E4, and ENA-1 (Fig. 5 *A*). The loss of binding of these three mAbs directly

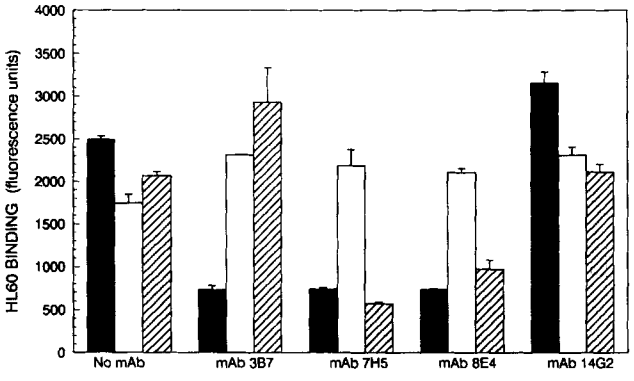

Figure 4. HL60 binding to HuRa-1 in the presence of blocking antibodies. Inhibition of HL60 binding to human E-selectin lec-egf-CD16 (■), rabbit E-selectin lec-egf-CD16 (□), and HuRa-1 human–rabbit chimeric E-selectin lectin-egf-CD16 (▨) transfected COS cells by anti–E-selectin blocking mAbs. Cells were preincubated with 3B7, 7H5, 8E4, or 14G2 (10 μg/ml) for 1 h and HL60 cell adhesion determined as described in Materials and Methods. Each bar represents the mean ± SD of triplicate determinations.

corresponded to the gain of binding demonstrated with the HuRa-1 chimera. Another NH_2-terminal mutation, E8A, was found to abolish the binding of BBA2 and ENA 1 (Fig. 5 *C*). Thus, in agreement with the human–rabbit chimera studies described above, residues at positions 7, 8, and 9 of the E-selectin lectin domain contribute to the epitopes recognized by four blocking mAbs.

Since the HuRa-2 chimera implicated residues 98 and 101 in binding of blocking antibody 3B7, the converse experiment was also done where the residues at these two sites in the E-selectin–IgG construct were replaced with their rabbit equivalents. The resultant mutant was found to not bind mAb 3B7 (Fig. 5 *B*), thus confirming the gain of binding found with HuRa-2. Finally, an E-selectin–IgG mutant which contained an alanine substitution at position 101 retained binding to mAb 3B7 (Table I), indicating that E98 was the crucial component of the 3B7 epitope.

The complexity of the epitope recognized by blocking mAb 7H5 is revealed by the mutation K113A (Fig. 5 *D*). This substitution, which is at the COOH terminus of the lectin do-

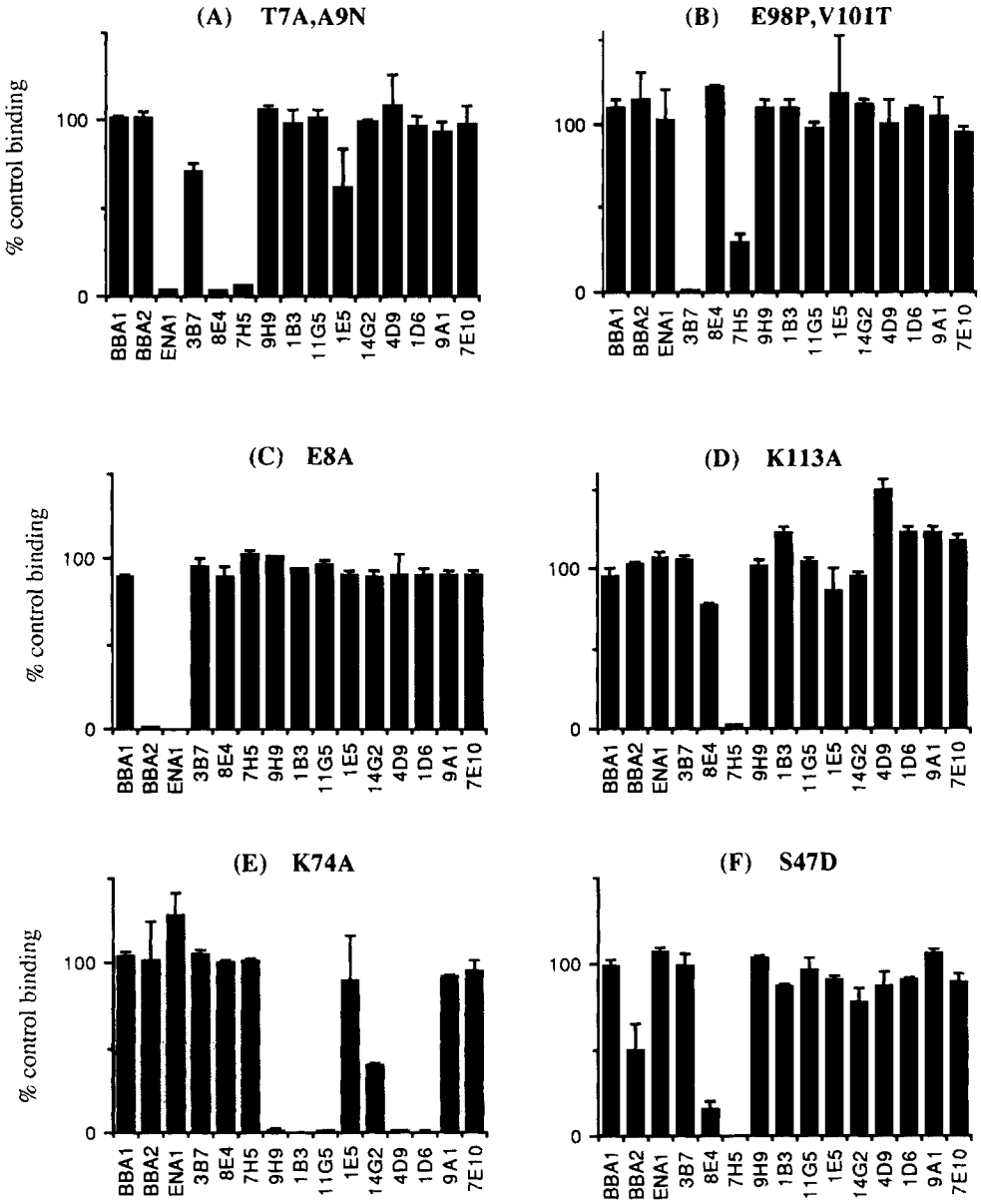

Figure 5. Reactivity of anti–E-selectin mAbs with mutant chimeras. E-selectin–IgG chimeras with the mutations shown were tested for capture by each of 15 mAbs using the ELISA format described in Materials and Methods. Results shown represent the mean ± SD of duplicate determinations and are expressed as percentage of control or wild-type binding.

Table I. E selectin-IgG Mutant Binding Summary

E selectin-IgG mutant	BBA1	BBA2	ENA1	3B7	8E4	7H5	mAb binding 9H9	1B3	11G5	1E5	14G2	4D9	1D6	9A1	7E10	sLEX binding
S2T N4H T5Y	+	+	+	+	+	+	+	+	+	+	+	+	+	+	+	+
T7A A9N	+	+	−	+	−	−	+	+	+	+	+	+	+	+	+	ND
E8A	+	−	−	+	+	+	+	+	+	+	+	+	+	+	+	+++
M10Y T11S Y12W	+	+	+	+	+	+	+	+	+	+	+	+	+	+	+	+
K32A	+	+	+	+	+	+	+	+	+	+	+	+	+	+	+	+
S43A	+	+	+	±	+	+	+	+	+	+	+	+	+	+	+	+
S45A	+	+	±	+	+	+	+	+	+	+	+	+	+	+	+	+
P46A	+	+	+	+	±	+	+	+	+	+	+	+	+	+	+	±
S47A	+	+	+	+	+	+	+	+	+	+	+	+	+	+	+	±
S47D	+	+	+	+	±	−	+	+	+	+	+	+	+	+	+	−
Y48F	+	+	+	+	+	+	+	+	+	+	+	+	+	+	+	−
K67A	+	+	+	+	+	+	+	+	+	+	+	+	+	+	+	+
K74A	+	+	+	+	+	+	−	−	−	+	±	−	−	+	+	+
R84A K86A	+	+	+	+	+	+	+	+	+	+	+	+	+	+	+	+
R97A	+	+	+	+	+	+	+	+	+	+	+	+	+	+	+	−
E98P V101T	+	+	+	−	+	±	+	+	+	+	+	+	+	+	+	ND
K99A	+	+	+	+	+	+	+	+	+	+	+	+	+	+	+	±
D100A	+	+	+	±	+	+	+	+	+	+	+	+	+	+	+	+
V101A	+	+	+	+	+	+	+	+	+	+	+	+	+	+	+	+
E107A	+	+	+	+	+	+	+	+	+	+	+	+	+	+	+	+
K111A	+	+	+	+	+	+	+	+	+	+	+	+	+	+	+	−
K113A	+	+	+	+	+	−	+	+	+	+	+	+	+	+	+	−
M10A	−	−	−	−	−	−	−	−	−	−	−	−	−	±	−	−
Y12A	−	−	−	−	−	−	−	−	−	−	−	−	−	±	−	−
E14A	not expressed															
Y44A	not expressed															
Y48A	+	+	±	±	±	±	±	±	±	±	±	±	±	+	±	ND
Y49A	−	−	−	−	−	−	−	−	−	−	−	−	−	−	−	ND
E92A	+	+	±	±	±	−	±	±	±	±	±	±	±	+	+	ND
I93A	ND	ND	ND	−	−	−	−	−	−	−	−	−	−	±	±	ND
Y94A	ND	ND	ND	−	−	−	−	−	−	−	−	−	−	−	−	ND
I95A	ND	ND	ND	−	−	−	−	−	−	−	−	−	−	−	−	ND
K96A	−	−	−	−	−	−	−	−	−	−	−	−	−	±	±	−
E98A	ND	ND	ND	−	−	−	−	−	−	−	−	−	−	±	±	ND
M103A	±	±	±	±	±	±	±	±	±	±	±	±	±	±	±	−
E14I, A15S, S16R, A17K	ND	ND	ND	−	−	−	−	−	−	−	−	−	−	−	−	ND
Y18A, Q20A, R22A	−	−	−	−	−	−	−	−	−	−	−	−	−	−	−	−
N39A, Y44A	−	−	−	−	−	−	−	−	−	−	−	−	−	−	−	−
R54A, K55A, N57A	−	−	−	−	−	−	−	−	−	−	−	−	−	±	±	−
K96A, R97A, K99A	−	−	−	−	−	−	−	−	−	−	−	−	−	−	−	−
K111S, K112A, K113A	−	−	−	−	−	−	−	−	−	−	−	−	−	−	−	−

+, Binding; ±, partial binding; −, no binding.

main, completely abolished 7H5 binding. Since 7H5 binding was also abolished by substitutions made at the NH_2 terminus of the lectin domain (positions 7 and 9, Fig. 5 *A*), this suggested that the epitope recognized by this blocking antibody is derived from both the NH_2 and COOH termini. Indeed, the partial loss of 7H5 binding found after substitution at residues 98 and 101 (Fig. 5 *B*) was consistent with close alignment of this region with the NH_2- and COOH-terminal sites recognized by this mAb as well. One interpretation of this result is that these regions may be closely aligned in the tertiary structure of the lectin domain (see below).

The binding of all of the nonblocking mAbs was not grossly affected by substitutions that disrupted blocking mAb recognition (Fig. 5, *A–D*). This was consistent with these two antibody classes recognizing distant sites in the lectin domain. For example, mutant K74A completely lost binding of a number of these nonblocking antibodies (9H9, 1B3, 11G5, 4D9, and 1D6) and partially lost binding of another (14G2) (Fig. 5 *E*). This substitution did not affect binding of any blocking mAbs, suggesting that this region is not directly involved in carbohydrate recognition.

Lastly, a number of amino acid substitutions resulted in the loss of binding to all of the antibodies in the panel, including 9A1 and 7E10, which recognize determinants in the complement-binding-like domains 1 and 2 of E-selectin. This result was obtained even though normalized amounts of these mutants, based upon human IgG concentrations, were added to the antibody-coated wells. These substitutions, therefore, appeared to have global effects on the recombinant E-selectin domains, and the apparent lack of mAb reactivity

could have been due to misfolding and/or degradation. These and other data on the binding of mAbs to various E-selectin mutants are summarized in Table I.

Carbohydrate Recognition by E-selectin Mutants

While the mAb-mapping data described above were consistent with the involvement of the NH_2 and COOH termini as well as the region surrounding residue 98 of the E-selectin lectin domain with carbohydrate recognition, the large "shadow" cast on an antigen by a bound antibody (typically 680–880 A^2) (15, 25) may cause blocking by steric hindrance of carbohydrate recognition sites relatively distant from the antibody epitope. Therefore, we analyzed the ability of a number of the E-selectin–IgG alanine mutants to bind sLe^x glycolipid (27) that had been immobilized on plastic microtitre wells. This assay has been validated previously (18), where the binding of the E-selectin–IgG chimera was shown to be calcium dependent, inhibited by E-selectin blocking mAbs and dependent upon the α2–3 sialic acid form of sLe^x.

As can be seen in Fig. 6 *A*, three different results were obtained with the various alanine substitutions analyzed. A number of substitutions did not affect the binding of E-selectin to immobilized sLe^x. These substitutions were found to be of the type that either did not affect the binding of any mAb (mutants K32A, K67A, and R84A, K86A) or affected binding of only nonblocking antibodies (mutant K74A). This result was consistent with the previously mentioned possibility that this region of E-selectin was not involved with carbohydrate recognition. Another effect was exemplified by mutations at positions R97, K99, and K113. Conversion of any of these sites to alanine either completely (R97 and K113) or almost completely (K99) abolished binding of E-selectin to sLe^x. While mutations at R97 and K99 had no effect on blocking antibodies binding, mutation at K113 completely abolished binding of blocking antibody 7H5 (see above). In addition, residue E98 (adjacent to R97 and K99) was crucial to the epitope of another blocking mAb, 3B7. These results unified the locations of blocking mAb epitopes with residues critical for carbohydrate recognition, and were consistent with the direct involvement of these regions of E-selectin with carbohydrate binding. The final, somewhat unexpected, effect of E-selectin mutation on sLe^x binding was exemplified by the E8A mutant. Fig. 6 *A* shows that this mutant appeared to show enhanced sLe^x binding when added at the same concentration as wild-type E-selectin chimera. A dose–response curve comparing E8A with wild-type E-selectin (Fig. 6 *B*) reveals that the mutant bound ~fivefold more avidly to sLe^x than wild type. This enhanced binding by E8A was completely calcium dependent and did not occur on the inactive α2–6 sialic acid form of the carbohydrate (data not shown). As described previously, substitutions in this region (i.e., at residues 7, 8, and 9) profoundly affect the binding of several blocking mAbs. Thus, it is likely that this region of E-selectin is also associated with ligand binding. Data on the ability of various E-selectin mutants to bind sLe^x are summarized in Table I.

A Model of the E-selectin Lectin Domain

While the results described above allow for a number of important conclusions about the regions of the E-selectin linear sequence involved in carbohydrate recognition, their relevance would be enhanced if they could be applied to a structural model of the lectin domain of this protein. In the absence of crystallographic data, a three-dimensional model of a molecule can be constructed using structural coordinates of related molecules (22). Recently, the x-ray structure of the

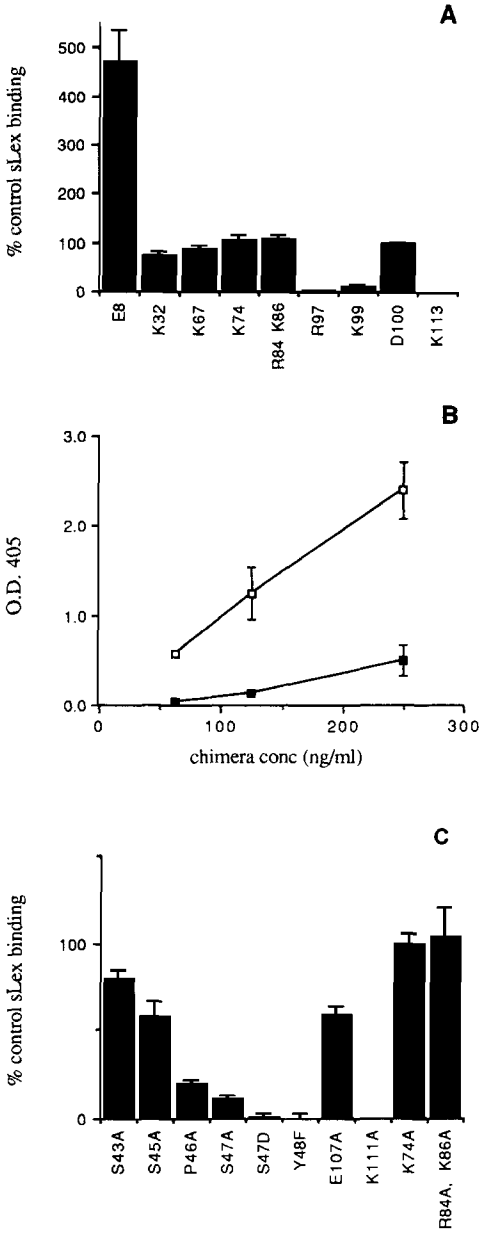

Figure 6. Binding of alanine mutants to immobilized sLe^x glycolipid. (*A*) E-selectin–IgG chimeras in which the indicated residues were mutated to alanine were tested for binding to immobilized 2,3 sLe^x glycolipid by the ELISA procedure described in Materials and Methods. Results shown represent the mean ± SD of triplicate determinations expressed as percentage of control or wild-type binding. (*B*) E-selectin–IgG mutant E8A (□) or wild-type E-selectin–IgG (■) were tested at the indicated concentrations for binding to immobilized 2,3 sLe^x glycolipid by ELISA as above. Results shown represent the mean ± SD of triplicate determinations. (*C*) E-selectin–IgG chimeras with the indicated mutations were tested for sLe^x binding as in *A*.

MBP, a type-C lectin that is homologous to the lectin domain of E-selectin, was determined (67). Therefore, to more fully understand the relative importance of the functional residues described above, we used these structural data to develop a model of the E-selectin lectin domain.

Derivation of the E-selectin model from the MBP coordinates was based on secondary structure common to both, encompassing 78 (of 121) E-selectin residues (67) (Fig. 7). Three models of E-selectin were evaluated, differing only in the conformation of two surface loops: S43-Y48 and Y94-D100, corresponding to MBP K152-S154 and V199-D200, respectively. The S43-Y48 loop contains a three residue insertion relative to MBP while the Y94-D100 loop contains a five residue insertion. The E-selectin model before energy minimization had a root-mean-square (r.m.s.) deviation of 0.17Å (78 Cα atoms) while that of the best energy-minimized model was 0.68Å. For comparative purposes, we also subjected the MBP crystal structure to the same energy-minimization regimen as used for E-selectin. The minimized MBP (molecule 1 only) showed a Cα r.m.s. deviation of 0.45Å (residues K110-C217, i.e., excluding seven NH_2- and COOH-terminal residues) versus the crystal structure. Hence the energy-minimization regimen maintained the secondary structure of the E-selectin model; this was accomplished by initially constraining the secondary structure Cα atoms and hydrogen bonds during minimization.

Weis et al. (67) noted the presence of small and large hydrophobic cores in MBP that were critical for overall structure. For the small core only two of six residues are conserved in E-selectin (G52, A115) though the model could accommodate the other four E-selectin sidechains without disturbing the protein fold. In the large core only 6 of 14 residues are conserved. One substitution, A155(MBP) to Y49(E-selectin), necessitated moving α-helix-2 (K32-L42) slightly away from the protein center to accommodate introduction of the Y49 sidechain. This tyrosyl side chain interacts with the two loops S43-Y48 and Y94-D100 mentioned above. At the opposite (NH_2 terminus) end of the helix, the substitution of P138(MBP) to I29(E-selectin) also contributed to the slight shift in α-helix-2. However, the substitutions in E-selectin in the large hydrophobic core fill the internal space created by the slight shift of α-helix-2. Thus, the relatively large number of amino acid changes in the hydrophobic core regions of MBP and the E-selectin lectin domain could be accommodated by the model.

The MBP crystal structure contains two putative Ca^{2+}-binding sites which, in the crystal structure, are occupied by two Holmium ions. As noted by Weis et al. (67), site 2 is retained in E-selectin: E80 Oε2, N82 Oδ1, E88 Oε2, N105 Oδ1, D106 Oδ2, D106 backbone carbonyl oxygen, and one water molecule coordinate this Ca^{2+}. The other Ca^{2+}-binding site is probably not present in the E-selectin lectin domain, also noted previously (67) (Fig. 7). While D89 (D194 in MBP) is conserved in E-selectin, D161 in MBP is replaced by K55 in E-selectin and two other sidechains which coordinate the MBP site 1 Ca^{2+}, i.e., E165 and D188, are replaced by N57 and N83 in E-selectin. While an Asn sidechain could still coordinate a Ca^{2+} via its Oδ1 atom, N57 is adjacent to a two residue deletion and the loop of which it is a part probably changes conformation. Likewise, N83 is part of a loop which has a proposed conformation in E-selectin different from that in MBP. Though this loop contains no insertions or deletions, the MBP sequence HGSG forms a Type II′ reverse turn with the Gly at position 4 having a backbone conformation allowable only for Gly (136°, 148°). The E-selectin sequence RQKD necessitated a different loop conformation due to the G to Q and G to D replacements. Thus, only one calcium binding site is predicted in the E-selectin lectin domain.

Of course, the most interesting aspect of this model is the location of the amino acid side chains whose mutation appeared to affect antibody binding and/or sLe^x recognition. As can be seen from the model (Fig. 7), the amino acid residues involved in blocking mAb recognition appear to form a patch on the surface of the lectin domain near the antiparallel beta sheet formed by the disulfide-linked NH_2 and COOH termini and the adjacent disulfide-linked loop formed by the two internal cysteines. Thus, amino acid side chains at positions 7, 8, 9, 98, and 113, all of which affected the binding of various blocking mAbs, are all found to be on the same face of E-selectin. Of particular importance was the relatively close proximity of the side chains of residues 7, 9, and 113 which was consistent with the effect of mutations at these residues on the binding of the 7H5 blocking mAb. The partial effect of mutation at residue 98 on 7H5 binding is also consistent with the model, since the loop containing this residue is found on the same face as residues 7, 9, and 113. The model also reveals that the side chain recognized by the nonblocking antibodies (K74) is found on a side of the lectin domain that is opposite to that which appears to bind the blocking antibodies (Fig. 7 *A*). This result is consistent with the region recognized by nonblocking antibodies being a considerable distance from the carbohydrate recognition site.

Examination of the location of amino acids found to affect sLe^x binding is consistent with the interpretation that the discrete structural region recognized by the blocking antibodies is in fact involved with carbohydrate recognition. All of the residues whose substitution affected sLe^x binding—E8, R97, K99, and K113—are found within this same region. Furthermore, the model suggests that a number of side chains whose mutation did not affect sLe^x binding may be located on a side of the molecule that is distinct from the apparent sLe^x binding site.

Mutations Based on Model Predictions

To test and refine the E-selectin model described above, we next introduced substitutions at additional residues predicted to comprise the face of E-selectin implicated in sugar binding. For example, the model predicts that the small loop from S43 to Y48 (in purple, Fig. 7 *B*) lies within the region defined by the blocking mAb and sLe^x binding studies. Consequently, mutagenesis of this loop (along with other residues in this region) was performed with the results shown in Fig. 6 *C* and summarized in Table I. Particularly noteworthy is the observation that mutation of K111 to alanine completely abolished sLe^x recognition (Fig. 6 *C*). Furthermore, mutation of residues within the S43-Y48 loop revealed that substitution at residues P46, S47 or Y48 decreased sugar binding. Whereas the substitution S47A significantly decreased sLe^x binding by E-selectin–IgG, the S47D mutation resulted in a complete loss of carbohydrate binding. Also, although the S47D mutant still bound mAb 3B7, this mutant bound blocking mAb 8E4 weakly and did not bind blocking

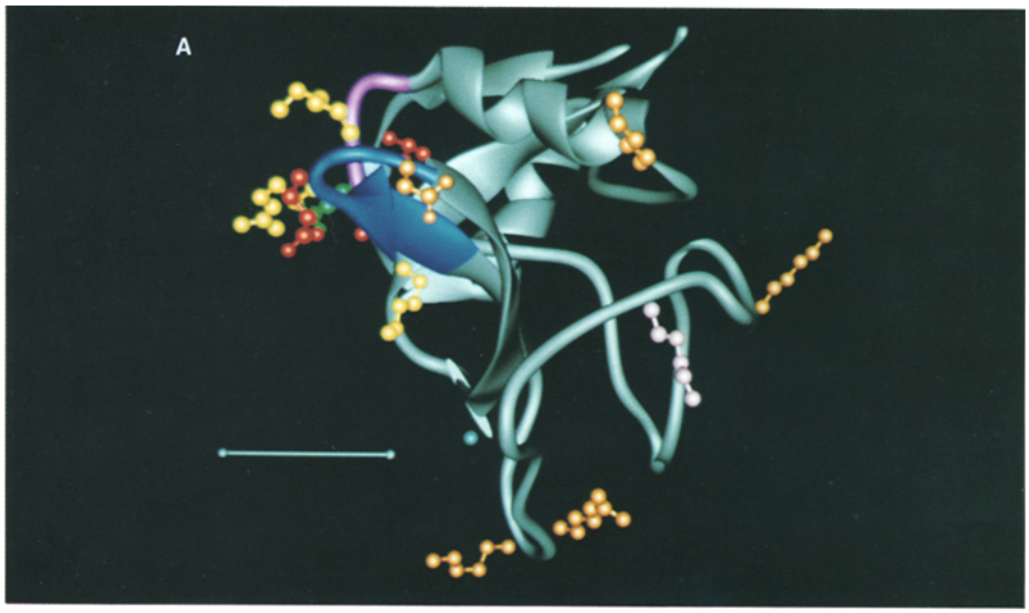
A

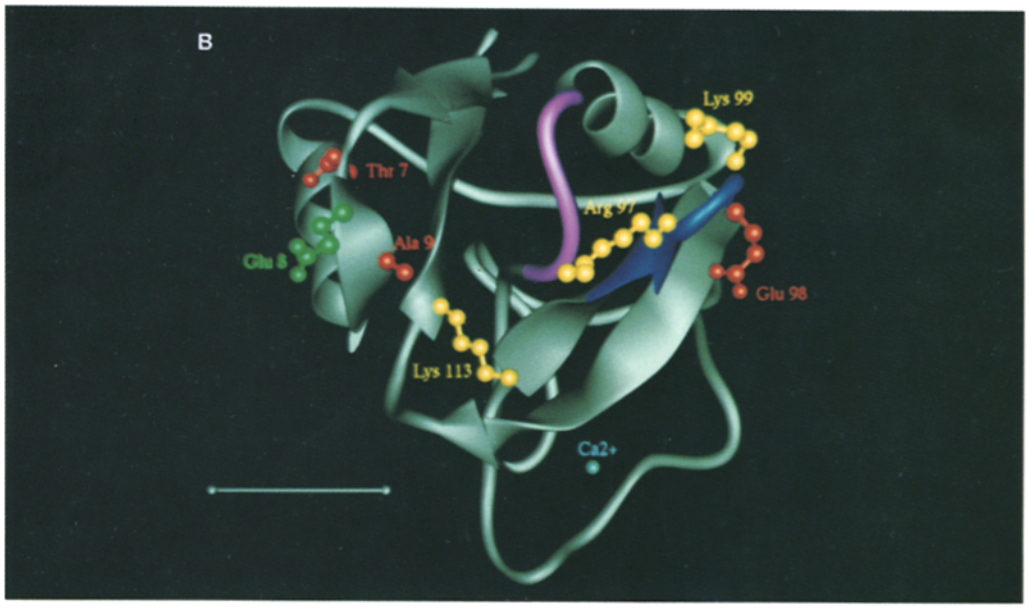
B
Lys 99
Thr 7
Arg 97
Glu 8
Ala 9
Glu 98
Lys 113
Ca2+

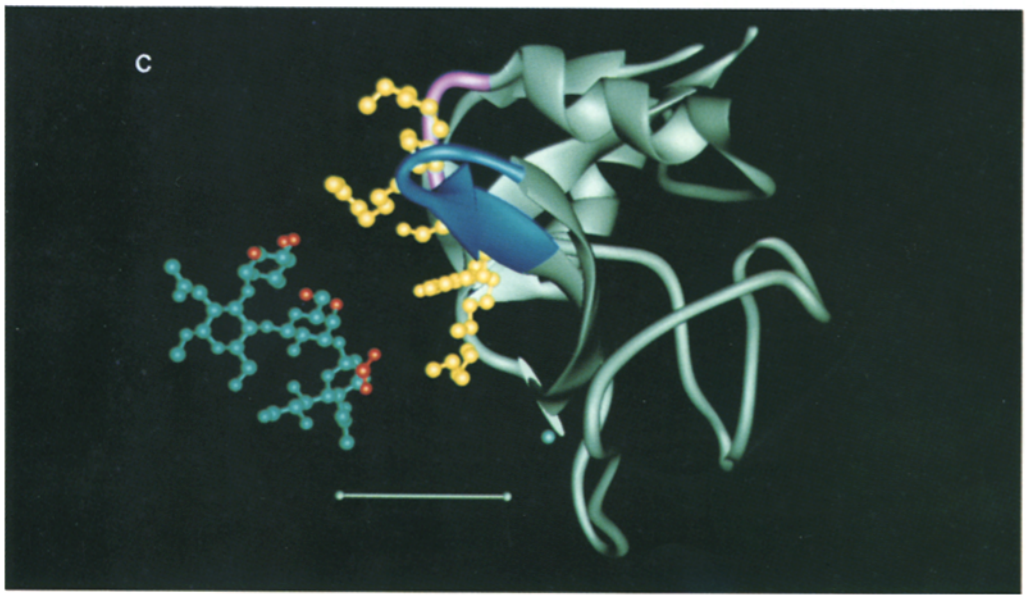
C

mAb 7H5 at all (Fig. 5 *F*). These results are consistent with the close alignment of this S43-Y48 loop with the aforementioned binding sites for 8E4 and 7H5, as was predicted by the model. Finally, since the substitution Y48A resulted in a misfolded protein (see Table I), Tyr 48 was replaced with phenylalanine to evaluate the contribution of this tyrosyl hydroxyl group to sLe^x recognition. This substitution did not affect recognition by any of the antibodies (Table I) but completely abolished carbohydrate binding (Fig. 6 *C*). Thus, further mutagenesis based on the model revealed additional components of the putative sLe^x binding site, all of which were entirely consistent with the predicted structure of the E-selectin lectin domain.

Discussion

The data reported here provide the first glimpse into the molecular interactions between E-selectin and its carbohydrate ligand, sLe^x. The work reported here is unique in that it combines the mapping of blocking and nonblocking mAb binding sites with the ability of a given E-selectin mutant to bind to a naturally occurring carbohydrate ligand, sLe^x. The agreement between blocking mAb mapping data and the location of mutations that affect sLe^x binding is consistent with the hypothesis that the small region of the E-selectin lectin domain identified here is directly involved with binding to the previously defined face of sLe^x (1, 58). This proposal is also supported by the fact that many nonblocking mAbs appear to map to the opposite side of the lectin domain. We therefore believe that we have identified an important carbohydrate recognition site on E-selectin.

One of the most interesting aspects of the mutagenesis described here is the discovery that three positively charged residues (R97, K111, and K113) that are critical for sLe^x recognition appear very close together on the E-selectin model (Fig. 7). A major supposition of the mutagenic analysis was based upon the potential importance of positively charged residues. The discovery that substitution of alanine for either of these side chains had profoundly negative effects on carbohydrate recognition supports the possibility that basic residues in selectin lectin domains are involved in carbohydrate recognition (34, 55, 69). One possible means by which this recognition could be accomplished is by charge interaction between these side chains and the carboxylate group of the sialic acid residue found in sLe^x. The importance of this carboxylate group is underlined by organic synthesis studies demonstrating that an sLe^x-like compound with a methyl ester on the sialic acid carboxylate is not effectively recognized by E-selectin (56, 58). Thus, it seems likely that some type of charge-mediated interaction may be involved with sLe^x adhesion to E-selectin. Since all three selectins require sialic acid for adhesion (10, 42, 46, 57, 58), it is interesting that, while K111 and K113 are found in all three selectins from a number of different species, a positively charged residue (R) is found at position 97 of L and E-selectin, while human P-selectin contains a serine at this site. The conservation of lysines at positions 111 and 113 of all selectins (33), together with the mutagenesis analysis described here, is consistent with a direct role for these residues in sialic acid recognition, perhaps by the formation of a salt bridge or hydrogen bond. The less stringent conservation between selectins at position 97 argues that this residue, while clearly involved with carbohydrate recognition, may have a less crucial role in sugar binding than residues K111 and K113. It is also interesting to note that S47 and Y48, which were implicated in sugar binding by the mutagenesis here, are conserved in all three selectins. The data reported here also implicate the NH_2 terminus of E-selectin in ligand binding. Mutagenesis of the NH_2 terminus was initially inspired by previous data that mapped the epitope for the blocking mAb Mel 14 to the NH_2 terminus of L-selectin (6). In agreement with that study, a number of anti-E-selectin blocking mAbs were found to recognize residues in the NH_2 terminus of this glycoprotein as well. In fact, of the five blocking antibodies that we have analyzed, four (BBA 2, ENA 1, 8E4, and 7H5) have been directly shown to bind to this region of E-selectin, consistent with a possible role for this site in binding and adhesion. The E8A mutation found to enhance carbohydrate binding is also consistent with the involvement of this site in sugar recognition, although the nature of this interaction is unclear (see below). However, the enhanced recognition of sLe^x by mutation at position 8 may be of biological significance. As was pointed out earlier, selectins appear to mediate a relatively low affinity "rolling" type of adhesion as a precursor to firmer adhesion mediated by leukocyte integrins (9, 36, 38, 59). It is possible that the NH_2-terminal region of E-selectin has evolved to decrease the relative affinity of carbohydrate recognition by incorporation of a relatively large side chain at this site. Accordingly, the other two selectins (L and P) contain a lysine at residue 8, and mutation of this lysine in L-selectin to an alanine similarly enhances sLe^x recognition by 5–10-fold (D. Erbe, unpublished data). It thus seems possible that a large, charged side chain at this site may serve to decrease the affinity of selectin–carbohydrate interactions.

Figure 7. A model of the lectin domain of E-selectin. Shown is a ribbon model of the E-selectin lectin domain derived from the published coordinates of the related type-C lectin, the mannose binding protein (67). Orientation *A* shows the amino acid residues whose mutation did not affect sLe^x or mAb binding (brown), the residue at position 74 whose mutation did not affect sLe^x binding but did affect binding of nonblocking mAbs (pink), the residues at positions 7,9, and 98 whose mutation abolished binding of blocking mAbs (red), the residues at positions 97, 99, 113 whose mutation abolished sLe^x binding (yellow), and the residue at position 8 whose mutation enhanced the affinity of E-selectin for sLe^x (green). As noted in the text, mutation of residues 8 and 113 also affected the binding of some blocking mAbs. The single bound calcium is depicted as a blue ball. Orientation *B* shows the "active site" of carbohydrate binding from a face-on view, with residues involved with carbohydrate recognition and/or blocking mAb binding colored as in orientation *A*. The purple loop (residues S43–Y48) and the dark blue loop (residues Y94–D100) denote two loops near the carbohydrate binding site of E-selectin that are not found in the MBP. Orientation *C* shows the E-selectin model as in *A* (but rotated slightly towards the viewer) with all of the residues whose mutation significantly decreased sLe^x binding shown in yellow (from top to bottom: K99, P46, R97, S47, Y48, K113, K111). For the purpose of relative size comparison, the solution structure of sLe^x is also shown with the known crucial carbohydrate moieties, the carboxylate of sialic acid, the 4 and 6 hydroxyls of galactose, and the 2, 3, and 4 hydroxyls of fucose (58), colored red. Bars, 10Å.

However, since the exact nature of the residue at position 8 (and those surrounding it) does not appear to be important (see Fig. 2) (33), it is unlikely that this residue is directly involved in sLe^x binding. Rather, this site may affect accessibility and/or flexibility of the sugar binding site.

While the other E-selectin residues delineated here may be directly involved with sLe^x recognition (see Fig. 7 *C*), indirect effects may also play a role in the loss of binding by some mutants. For example, The K99A substitution may have affected sLe^x binding indirectly by changing the Y94-D100 loop conformation such that R97 no longer formed a stable contact with the carbohydrate. In fact, when this K99A mutant IgG chimera was tested in an HL60 cell binding assay, it mediated adhesion comparable to wild-type E-selectin-IgG, while the R97A, K111A, and K113A mutants were completely negative for HL60 cell binding (B. Wolitzky, unpublished data). This result is consistent with the possibility that the K99A substitution affects sLe^x binding indirectly. A similar situation may occur in which the P46A substitution affects the S43-Y48 loop such that S47 and/or Y48 no longer contact the sugar. Another indirect effect of these mutations might involve interactions between the EGF and lectin domains. Previous data have clearly demonstrated a role for the EGF domain in mediation of lectin domain structure in selectins (6, 60). However, it must be emphasized that the retention of mAb binding to the mutants described here is not consistent with the structural disruptions expected after loss of interaction between the lectin and EGF domains (6, 60). Lastly, mutagenesis of the mannose binding protein indicated that some substitutions resulted in a decreased affinity for calcium and a subsequent loss of sugar binding. Higher calcium levels restored mannose binding by these mutants (47a). However, the E-selectin mutants described here still did not bind sLe^x at calcium concentrations as high as 20 mM (B. Brandley, unpublished data). Therefore, our results are most consistent with a direct role for at least R97, K111, and K113, and perhaps S47 and Y48, in sLe^x binding by E-selectin (see Fig. 7 *C*).

Recently, Geng and co-workers showed that a mAb capable of inhibiting neutrophil binding to P-selectin mapped to residues 19–34 of this molecule, and that a peptide corresponding to this stretch also inhibited neutrophil binding to P-selectin (21). In the model of E-selectin presented here, residues 19–34 form a loop which is on the opposite side from the site where sLe^x appears to bind. The two mutants made within this sequence in E-selectin either did not affect sLe^x or mAb binding (mutant K32A) or resulted in a misfolded protein (Mutant Y18A, Q20A, R22A). Thus our data are not consistent with the direct involvement of this region in carbohydrate recognition by E-selectin, although an extensive mutational analysis of this loop was not performed.

Recognition of cell surface carbohydrates by selectins is one of the most important events during normal and pathogenic inflammatory responses. The data reported in this paper provide a preliminary view of some of the molecular interactions that mediate this type of adhesion. While the ultimate depiction of the association between a ligand and receptor requires crystallization of the complexes formed between them, mutagenic investigations similar to that reported here have been found to give a highly informative representation of the true nature of ligand–receptor interactions (12, 13, 14, 16, 68). Furthermore, the work described here should complement crystallographic analysis by indicating which residues at the protein–carbohydrate interface contribute most to binding energy. Perhaps the greatest use of the E-selectin model described herein will be to focus further structure/function studies aimed at the design of carbohydrate-based inhibitors of E-selectin/sLe^x binding. It is hoped that such drugs may ultimately find use as effective inhibitors of inflammatory responses mediated by selectins.

We thank Dr. William Weis for providing the MBP coordinates before publication; Drs. Michael Quesenberry and Kurt Drickamer for providing MBP mutagenesis data before publication; Drs. Mark Zoller, Craig Gibbs, Jim Wells and Don Dowbenko for advice and discussion; Dr. Ann Goldstein for human umbilical vein endothelial cells; Dr. K. S. Huang for purified recombinant E-selectin; Dr. Brian Seed for human E-selectin cDNA; and Dr. Bradford Graves for helpful discussions on E-selectin structure and modeling.

Received for publication 21 May 1992.

References

1. Berg, E. L., M. K. Robinson, O. Mansson, E. C. Butcher, and J. L. Magnani. 1991. A carbohydrate domain common to both sialyl Le^a and sialyl Le^x is recognized by the endothelial cell leukocyte adhesion molecule ELAM-1. *J. Biol. Chem.* 265:14869–14872.
2. Bernstein, F. C., T. F. Koetzle, G. J. B. Williams, E. F. Meyer, Jr., M. D. Brice, J. R. Rodgers, O. Kennard, T. Shimanouchi, and M. Tasumi. 1977. The protein databank: a computer-based archival file for macromolecular studies. *J. Mol. Biol.* 112:535–542.
3. Bevilacqua, P. P., J. S. Pober, D. L. Mendrick, R. S. Cotran, and M. A. Gimbrone, Jr. 1987. Identification of an inducible endothelial-leukocyte adhesion molecule. *Proc. Nat. Acad. Sci. USA.* 84:9238–9242.
4. Bevilacqua, M. P., S. Stengelin, M. A. Gimbrone, Jr., and B. Seed. 1989. Endothelial leukocyte adhesion molecule 1: an inducible receptor for neutrophils related to complement regulatory proteins and lectins. *Science (Wash. DC).* 243:1160–1165.
5. Bonfanti, R., B. Furie, B. Furie, and D. Wagner. 1989. PADGEM is a component of Weibel-Palade bodies in endothelial cells. *Blood.* 73: 1109–1112.
6. Bowen, B., C. Fennie, and L. A. Lasky. 1990. The Mel-14 antibody binds to the lectin domain of the murine peripheral lymph node homing receptor. *J. Cell Biol.* 107:1853–1862.
7. Branden, C., and J. Tooze. 1991. Introduction to Protein Structure. Garland Publishing, Inc., New York. 262–263.
8. Brandley, B., S. Swiedler, and P. Robbins. 1990. Carbohydrate ligands for the LEC cell adhesion molecules. *Cell.* 63:861–863.
9. Butcher, E. C. 1991. Leukocyte-endothelial cell recognition: three (or more) steps to specificity and diversity. *Cell.* 67:1033–1036.
10. Corrall, L., M. Singer, B. Macher, and S. Rosen. 1990. Requirement for sialic acid on neutrophils in a gmp140(PADGEM) mediated adhesive interaction with activated platelets. *Biochem. Biophys. Res. Commun.* 172: 1349–1352.
11. Cullen, B. R. 1987. Use of eukaryotic expression technology in the functional analysis of cloned genes. *In* Methods in Enzymology. S. L. Berger and A. R. Kimmel, editors. Academic Press, New York. 152:684–704.
12. Cunningham, B. C., and J. A. Wells. 1989. High-resolution epitope mapping of hGH-receptor interactions by alanine-scanning mutagenesis. *Science (Wash. DC).* 244:1081–1085.
13. Cunningham, B. C., P. Jhurani, P. Ng, and J. A. Wells. 1989. Receptor and antibody epitopes in human growth hormone identified by homolog-scanning mutagenesis. *Science (Wash. DC).* 243:1330–1336.
14. Cunningham, B. C., M. Ultsch, A. M. de Vos, M. G. Mulkerrin, K. R. Clauser, and J. A. Wells. 1991. Dimerization of the extracellular domain of the human growth hormone receptor by a single hormone molecule. *Science (Wash. DC).* 254:821–825.
15. Davies, D. R., and E. A. Padlan. 1990. Antibody-antigen complexes. *Annu. Rev. Biochem.* 59:439–473.
16. de Vos, A. M., M. Ultsch, and A. A. Kossiakoff. 1992. Human growth hormone and extracellular domain of its receptor: crystal structure of the complex. *Science (Wash. DC).* 255:306–312.
17. Fersht, A. R., J.-P. Shi, J. Knill-Jones, D. M. Lowe, A. J. Wilkinson, D. M. Blow, P. Brick, P. Carter, M. M. Y. Waye, and G. Winter. 1985. Hydrogen bonding and biological specificity analyzed by protein engineering. *Nature (Lond.).* 314:235–238.
18. Foxall, C., S. Watson, D. Dowbenko, C. Fennie, L. Lasky, M. Kiso, A. Hasegawa, D. Asa, and B. Brandley. 1992. The three members of the selectin receptor family recognize a common carbohydrate epitope, the sialyl Lewis X oligosaccharide. *J. Cell Biol.* 117:895–902.
19. Galfre, G., S. C. Howe, C. Milstein, G. W. Butcher, and J. C. Howard. 1977. Antibodies to major histocompatibility antigens produced by hybrid cell lines. *Nature (Lond.).* 266:550–552.

20. Gallatin, M., I. Weissman, and E. Butcher. 1983. A cell-surface molecule involved in organ-specific lymphocyte homing. *Nature (Lond.).* 303: 30–34.
21. Geng, J.-G., K. L. Moore, A. E. Johnson, and R. P. McKever. 1991. Neutrophil recognition requires a Ca^{2+}-induced conformational change in the lectin domain of GMP-140. *J. Biol. Chem.* 266:22313–22318.
22. Greer, J. 1981. Comparative model-building of the mammalian serine proteases. *J. Mol. Biol.* 153:1027–1042.
23. Hoogenraad, N. J., and C. J. Wraight. 1986. The effect of pristane on ascites tumor formation and monoclonal antibody production. *Methods Enzymol.* 121:375–381.
24. Imai, Y., M. S. Singer, C. Fennie, L. A. Lasky, and S. D. Rosen. 1991. Identification of a carbohydrate-based endothelial ligand for a lymphocyte homing receptor. *J. Cell Biol.* 113:1213–1221.
25. Jin, L., B. Fendley, and J. A. Wells. 1992. High resolution functional analysis of antibody-antigen interaction. *J. Mol. Biol.* In press.
26. Johnson, G. I., R. G. Cook, and R. P. McEver. 1989. Cloning of GMP-140, a granule membrane protein of platelets and endothelium: sequence similarity to proteins involved in cell adhesion and inflammation. *Cell.* 56:1033–1044.
27. Kameyama, A., H. Ishida, M. Kiso, and A. Hasegawa. 1991. Total synthesis of sialyl Lewis X. *Carbohydr. Res.* 209:c1–c4.
28. Kuijpers, T. W., B. C. Hakkert, M. Hoogerwerf, J. F. M. Leuuwenberg, and D. Roos. 1991. Role of endothelial leukocyte adhesion molecule-1 and platelet activating factor in neutrophil adherence to IL-1 prestimulated endothelial cells. *J. Immunol.* 147:1369–1376.
29. Kunkel, T. A., J. D. Roberts, and R. A. Zakour. 1987. Rapid and efficient site-specific mutagenesis without phenotypic selection. *Methods Enzymol.* 154:367–382.
30. Larigan, J. D., T. C. Tsang, J. M. Rumberger, and D. K. Burns. 1992. Characterization of cDNA and genomic sequences encoding rabbit ELAM-1: conservation of structure and functional interaction with leukocytes. *J. DNA Cell Biol.* 11:149–162.
31. Larsen, E., A. Celi, G. Gilbert, B. Furie, J. Erban, R. Bonfanti, D. Wagner, and B. Furie. 1989. PADGEM protein: a receptor that mediates the interaction of activated platelets with neutrophils and monocytes. *Cell.* 59:305–312.
32. Larsen, E., T. Palabrica, S. Sajer, G. E. Gilbert, D. D. Wagner, B. C. Furie, and B. Furie. 1990. PADGEM-dependent adhesion of platelets to monocytes and neutrophils is mediated by a lineage-specific carbohydrate, LNF III (CD15). *Cell.* 63:467–474.
33. Lasky, L. A. 1991. Lectin Cell Adhesion Molecules (LEC-CAMS): a new family of cell adhesion proteins involved with inflammation. *J. Cell Biochem.* 45:139–146.
34. Lasky, L. A., M. S. Singer, T. A. Yednock, D. Dowbenko, C. Fennie, J. Rodriguez, T. Nguyen, S. Stachel, and S. D. Rosen. 1989. Cloning of a lymphocyte homing receptor reveals a lectin domain. *Cell.* 56: 1045–1055.
35. Lasky, L. A., M. Singer, D. Dowbenko, Y. Imai, W. Henzel, C. Grimley, C. Fennie, N. Gillett, S. Watson, and S. D. Rosen. 1992. An endothelial ligand for L-selectin is a novel mucin-like molecule. *Cell.* 69:927–938.
36. Lawrence, M. B., and T. A. Springer. 1991. Leukocyte roll on a selectin at physiologic flow rates: distinction from and prerequisite for adhesion through integrins. *Cell.* 65:859–873.
37. Leeuwenberg, J. F. M., G. M. A. A. Jeunhomme, and W. A. Buurman. 1990. Adhesion of polymorphonuclear cells to human endothelial cells. Adhesion-molecule-dependent, and Fc-receptor-mediated adhesion-molecule-independent mechanisms. *Clin. Exp. Immunol.* 81:496–500.
38. Ley, K., P. Gaehtgens, C. Fennie, M. Singer, L. A. Lasky, and S. Rosen. 1991. Lectin-like cell adhesion molecule 1 mediates leukocyte rolling in mesenteric venules in vivo. *Blood.* 77(12):2553–2555.
39. Lowe, J. B., L. M. Stoolman, R. P. Nair, R. D. Larsen, T. L. Berhend, and R. M. Marks. 1990. ELAM-1-dependent cell adhesion to vascular endothelial cell determined by a transfected human fucosyltransferase cDNA. *Cell.* 63:475–484.
40. Luscinskas, F. W., A. F. Brock, M. A. Arnaout, and M. A. Gimbrone, Jr. 1989. Endothelial leukocyte adhesion molecule-1 dependent and leukocyte (CD11/18)-dependent mechanisms contribute to polymorphonuclear leukocyte adhesion to cytokin-activated human vascular endothelium. *J. Immunol.* 142:2257–2263.
41. McEver, R., J. Beckstead, K. Moore, L. Marshall-Carlson, and D. Bainton. 1989. GMP-140, a platelet alpha granule membrane protein, is also synthesized by vascular endothelial cells and is localized in Weibel-Palade bodies. *J. Clin. Invest.* 84:92–99.
42. Moore, K. L., A. Varki, and R. P. McEver. 1991. GMP-140 binds to a glycoprotein receptor on human neutrophils: evidence for a lectin-like interaction. *J. Cell Biol.* 112:491–499.
43. Phillips, M. L., E. Nudelman, F. C. A. Gaeta, M. Perez, A. K. Singhai, S. Hakomori, and J. C. Paulson. 1990. ELAM-1 mediates cell adhesion by recognition of a carbohydrate ligand, sialyl-Le^x. *Science (Wash. DC).* 250:1130–1132.
44. Picker, L. J., T. K. Kishimoto, C. W. Smith, R. A. Warnock, and E. C. Butcher. 1991. ELAM-1 is an adhesion molecule for skin-homing T cells. *Nature (Lond.).* 349:796–799.
45. Pigott, R., L. Needham, R. Edwards, C. Walker, and C. Power. 1991. Structural and functional studies of the endothelial activation antigen endothelial leukocyte adhesion molecule 1 using a panel of monoclonal antibodies. *J. Immunol.* 147:130–135.
46. Polley, M. J., M. L. Phillips, E. Wayner, E. Nudelman, A. K. Singhai, S. Hakomori, and J. C. Paulson. 1991. CD62 and endothelial cell-leukocyte adhesion molecule 1 (ELAM-1) recognize the same carbohydrate ligand, sialyl-Lewis x. *Proc. Natl. Acad. Sci. USA.* 88:6224–6228.
47. Ponder, J. W., and F. M. Richards. 1987. Tertiary template for proteins of packing criteria in the enumeration of allowed sequences for different structural classes. *J. Mol. Biol.* 193:775–791.
47a. Quesenberry, M. S., and K. Drickamer. 1992. Role of conserved and nonconserved residues in the Ca^{2+}-dependent carbohydrate-recognition domain of a rat mannose-binding protein: analysis by random cassette mutagenesis. *J. Biol. Chem.* 267:10831–10841.
48. Reik, L. M., S. L. Maines, D. E. Ryan, W. Levin, S. Bandiera, and P. E. Thomas. 1987. A simple, non-chromatographic purification procedure for monoclonal antibodies. Isolation of monoclonal antibodies against cytochrome P 450 isoenzymes. *J. Immunol. Methods.* 100:123.
49. Scallon, B. J., S. Scigliano, V. H. Freedman, M. C. Miedel, Y-C. E. Pan, J. C. Unkeless, and J. P. Kochan. 1989. A human immunoglobulin G receptor exists in both polypeptide-anchored and phosphatidylinositol-glycan anchored forms. *Proc. Natl. Acad. Sci. USA.* 86:5079–5083.
50. Shimizu, Y., S. Shaw, N. Graber, T. V. Gopal, K. J. Horgan, G. A. Van Seventer and W. Neuwman, 1991. Activation-independent binding of human memory T cells to adhesion molecule ELAM-1. *Nature (Lond.).* 349:799–802.
51. Siegelman, M., M. Van de Rijn, and I. Weissman. 1989. Mouse lymph node homing receptor cDNA clone encodes a glycoprotein revealing tandem interaction domains. *Science (Wash. DC).* 243:1165–1172.
52. Smith, A. L., and D. C. Benjamin. 1991. The antigenic surface of *Staphylococcal* nuclease II. Analysis of the N-1 epitope by site-directed mutagenesis. *J. Immunol.* 146:1259–1264.
53. Springer, T., and L. A. Lasky. 1991. Sticky sugars for selectins. *Nature (Lond.).* 349:196–197.
54. Stoolman, L. M. 1989. Adhesion molecules controlling lymphocyte migration. *Cell.* 56:907–910.
55. Stoolman, L., T. Tenforde, and S. Rosen. 1984. Phosphomannosyl receptors may participate in the adhesive interactions between lymphocytes and high endothelial venules. *J. Cell Biol.* 99:1535–1540.
56. Tiemyer, M., S. J. Swiedler, M. Ishihara, M. Moreland, H. Schweingruber, P. Hirtzer, and B. K. Brandley. 1991. Carbohydrate ligands for endothelial-leukocyte adhesion molecule 1. *Proc. Natl. Acad. Sci. USA.* 88:1138–1142.
57. True, D. D., M. S. Singer, L. A. Lasky, and S. D. Rosen. 1990. Requirement for sialic acid on the endothelial ligand of a lymphocyte homing receptor. *J. Cell Biol.* 111:2757–2764.
58. Tyrrell, D., P. James, N. Rao, C. Foxall, S. Abbas, F. Dasgupta, M. Nashed, A. Hasegawa, M. Kiso, D. Asa, J. Kidd, and B. K. Brandley. 1991. Structural requirements for the carbohydrate ligand of E-selectin. *Proc. Natl. Acad. Sci. USA.* 88:10372–10376.
59. Von Andrian, U., J. Chambers, L. McEvoy, R. Bargatze, K. Arfors, and E. Butcher. 1991. Two-step model of leukocyte-endothelial cell interaction of inflammation: distinct roles for LECAM-1 and the leukocyte beta 2 integrins in vivo. *Proc. Natl. Acad. Sci. USA.* 88:1538–1542.
60. Walz, G., A. Aruffo, W. E. Kolanus, M. Bevilacqua, and B. Seed. 1990. Recognition by ELAM-1 of the sialyl-Lex determinant on myeloid and tumor cells. *Science (Wash. DC).* 250:1132–1135.
61. Watson, S. R., Y. Imai, C. Fennie, J. S. Geoffroy, S. D. Rosen and L. A. Lasky. 1990. A homing receptor IgG chimera as a probe for adhesive ligands of lymph node high endothelial venules. *J. Cell Biol.* 110:2221–2229.
62. Watson, S. R., C. Fennie, and L. A. Lasky. 1991. Neutrophil influx into an inflammatory site inhibited by a soluble homing receptor-IgG chimaera. *Nature (Lond.).* 349:164–167.
63. Watson, S. R., Y. Imai, C. Fennie, J. Geoffroy, M. Singer, S. D. Rosen, and L. A. Lasky. 1991. The complement binding-like domains of the murine homing receptor facilitate lectin activity. *J. Cell Biol.* 115:235–243.
64. Weiner, S. J. , P. A. Kollman, D. A. Case, U. C. Singh, C. Ghio, G. Alagona, S. Profeta, Jr., and P. Weiner. 1984. A new force field for molecular mechanical simulation of nucleic acids and proteins. *J. Am. Chem. Soc.* 106:765–784.
65. Weiner, S. J., P. A. Kollman, D. T. Nguyen, and D. A. Case. 1986. An all atom force field for simulations of proteins and nucleic acids. *J. Comp. Chem.* 7:230–252.
66. Weis, W., J. H. Brown, S. Cusack, J. C. Paulson, J. J. Skehel, and D. C. Wiley. 1988. Structure of the influenza virus haemagglutinin complexed with its receptor, sialic acid. *Nature (Lond.).* 333:426–431.
67. Weis, W., R. Kahn, R. Fourme, K. Drickamer, and W. Hendrickson. 1991. Structure of the calcium-dependent lectin domain from a rat mannose-binding protein determined by MAD phasing. *Science (Wash. DC).* 254:1608–1615.
68. Wells, J. A. 1991. Systematic mutational analysis of protein-protein interfaces. *Methods Enzymol.* 202:390–410.
69. Yednock, T. A., L. M. Stoolman, and S. D. Rosen. 1987. Phosphomannosyl-derivatized beads detect a receptor involved in lymphocyte homing. *J. Cell Biol.* 104:713–723.